Rare Metal Materials and Engineering
Volume 48, Issue 11, November 2019
Available online at www.rmme.ac.cn

Science Press

Cite this article as: Rare Metal Materials and Engineering, 2019, 48(11): 3441-3447.

ARTICLE

Microstructure and Wear Behavior of Hard Ni60 and Soft WC-12Co/Ni25 Coatings Prepared by Laser Cladding on W1813N Non-magnetic Stainless Steel

Yang Lijing, Zhang Pingxiang, Wang Shaopeng, Li Zhengxian, Wang Pei, Li Huan, Yang Haiyu

Northwest Institute for Nonferrous Metal Research, Xi'an 710016, China

Abstract: The hard Ni60 (60HRC) self-fluxing alloy powder and soft Ni25-based WC-12Co composite powder were separately deposited onto the W1813N non-magnetic stainless steel using laser cladding (LC). The microstructure, phase composition and worn track characteristics of the Ni60 coating and WC-12Co/Ni25 composite coating were analyzed using scanning electron microscopy (SEM), energy dispersive spectrum (EDS), X-ray diffraction (XRD) and a step profiler. The micro-hardness, friction coefficient, profile of worn track and wear mechanism of both coatings were investigated. The results show that the microstructure is mainly fine dendrite and equiaxed crystal in the LC Ni60 coating, and the hard $Cr_{23}C_6$ and Cr_2B phases are distributed in the grain boundary of γ-Ni and FeNi solid solution, while WC-12Co particles in the composite coating are uniformly embedded in the Ni25 matrix, and the volume fraction of WC-12Co in the composite coating is 32.5 vol%. The difference value between minimum and maximum hardness in the WC-12Co/Ni25 composite coating reaches 6480 MPa. Although the mean friction coefficients of both coatings are similar, the volume loss of the LC WC-12Co/Ni25 is only 10% of that of the LC Ni60. The surface abrasive behaviors of the LC Ni60 coating are ploughed shape and adhesive scraps, but the surface abrasive behaviors of the LC WC-12Co/Ni25 composite coating are adhesive scraps and WC debris. The wear mechanism of the Ni60 coating is abrasive wear and adhesive wear, while the wear mechanism of the WC-12Co/Ni25 coating is adhesive wear. These demonstrate that the WC-12Co/Ni25 coating exhibits better wear resistance than the LC Ni60.

Key words: nickel-based alloy; WC-12Co ceramics; laser cladding, composite coating; wear resistance

W1813N non-magnetic stainless steel is widely used in the oil drilling exploration industry. However, the poor wear resistance of W1813N steel restricts its service life in drilling applications. Surface coating technology is an effective approach for preparing a wear-resistant layer on W1813N steel substrate by thermal spray or laser cladding. In thermal spray process, plasma jets or process gasses are used to melt or partially melt the particles and to accelerate the powder to impact a substrate, and the interface bonding mechanism is mainly mechanical bond between coating and substrate, so the thermal spray coating is possible to fall off and to crack under impact load[1-3]. However, compared with thermal spray, in laser cladding (LC) process, high energy laser beam is used to melt feedstock material and the surface layer of the substrate, resulting in the coating/substrate metallurgical bonding[4, 5]. Therefore, the laser cladding technology is a better choice to improve the wear resistance of W1813N steel.

In traditional industry applications, hardness is the most important indicator for evaluating the wear resistance of metal material. With the improvement of wear resistance, the composite material coating is researched. At present, it is not clear which of a single hard metal coating and a soft metal-based ce-

Received date: November 18, 2018
Foundation item: National Natural Science Foundation of China (51701165); China Postdoctoral Science Foundation (2017M623334XB); Natural Science Foundation of Shaanxi Province (2018JM5005); Shaanxi Postdoctoral Science Foundation (2018BSHQYXMZZ36)
Corresponding author: Yang Lijing, Ph. D., Senior Engineer, Northwest Institute for Nonferrous Metal Research, Xi'an 710016, P. R. China, E-mail: yanglijing84@126.com

ramics composite coating has better wear resistance. In this paper, the nickel-based self-fluxing alloy powder and WC-12Co ceramics are selected as wear-resistant coating material. Ni-based self-fluxing alloy is Ni-Cr-Si-B series metal material. Adding Cr elements in a Ni-based alloy can generate solution strengthening of γ-Ni matrix and improve the corrosion resistance and high temperature oxidation resistance, and excessive Cr in Ni-based alloy can react with C and B elements to form hard phases such as CrB, Cr_7C_3, $Cr_{23}C_7$, which will significantly enhance the wear resistance of Ni-based alloy[6,7]. Tungsten carbide (WC) is one of the most important enhancing materials, which is widely added as a hard phase in the abrasive coating. WC ceramics have some unique properties such as high melting point (2600 °C), high hardness, red hardness and good wettability to Co, Fe and Ni metals, except poor high temperature oxidation resistance and friability[8, 9]. In order to restrain the oxidation of WC and to enhance the adhesive force between WC and metal matrix, adding Co metal in WC can produce the WC-Co powder by sintering and pulverizing.

In the present applied research about laser cladding, Ni-based alloy and WC are most commonly used cladding abrasive materials. Nevertheless, researchers seldom discuss the distinction in wear resistance of hard metal coating and soft metal-based WC composite coating. Wang et al[10] prepared hard Ni60 cladding layers added with different amounts of rare-earth CeO_2, Y_2O_3, and La_2O_3 on the surface of 6063 aluminum alloys through laser cladding. Yao et al[11] studied the wear resistance of hard Ni60 alloy coatings deposited by laser cladding and laser assisted cold spray. These results show that the Ni60 coating prepared by laser cladding possesses excellent abrasive resistance and high temperature oxidation resistance. Sui et al[12] fabricated the Ni35+WC, Ni35+original sialon powders (OSP), and Ni35+WC+OSP composite coatings by laser cladding on 45 steel downhole tools. In order to improve the distribution and bonding strength of WC particles in composite coatings, Shu and Yao[13, 14] et al studied that in situ synthesized high volume fraction WC reinforced Ni-based composite coating and pre-alloyed WC-NiCrMo powder are deposited on a mild steel and SS316L substrate by high power diode laser. Ma et al[15] reported the effects of Ti elements on microstructure homogenization and properties of Ni60/WC composite coatings which were fabricated by wide-band laser cladding. Deschuyteneer et al[16] discussed that NiCrBSi/WC composite coatings containing various amounts of WC/W_2C particles are clad on low carbon steel substrate S235JR using a 1 kW Nd:YAG and a 3.8 kW high power diode laser. These researches indicate that hard Ni-based alloy powder and Ni-based WC composite powder are appropriate for preparing wear-resistant materials by laser cladding.

The aim of this study is to explore an effective and economical way for improving the service life of wear resistant components. In this research, hard Ni60 (60HRC) self-fluxing alloy powder and Ni25/WC-12Co composite powder were deposited onto the W1813N non-magnetic stainless steel using laser cladding. Comparison of the microstructure, phase and wear resistance between hard Ni60 coating and WC-12Co/Ni25 composite coating reveals that which one of single hard metal coating and adding ceramic particles in the coating is more effective in improving the wear resistance of coating.

1 Experiment

W1813N steel (0Cr13Mn18Ni2MoN) was used as the substrate (100 mm× 50 mm× 10 mm) and the surface of substrate was prepared by blasting using ~325 mesh Al_2O_3. Commercially available hard nickel-based self-fluxing Ni60 alloy powder and soft Ni25 and WC-12Co powders were used to fabricate the LC Ni60 and WC-12Co/Ni25 coatings. The WC-12Co particles and Ni-based alloy powder (Ni60, Ni25) are irregular and spherical, whose average sizes are in the range of 40~50 and 20~50 μm, respectively. The WC-12Co powder was prepared by sintering and pulverizing, whose chemical composition and morphology are shown in Fig.1a. The morphologies of Ni60 and Ni25 powder prepared by gas atomization are similar, whose chemical compositions are given in Table 1. The WC-12Co/Ni25 composite powders are composed of 40 wt% WC-12Co and 60 wt% Ni25.

The coatings were fabricated using a continuous wave CO_2 laser (HANSGS-TFL-10000) processing system with a maximum power of 10 kW. The powder was introduced into the beam with a coaxial powder-feed system. The carrier gas of powder-feed and the shielding gas of molten pool were argon.

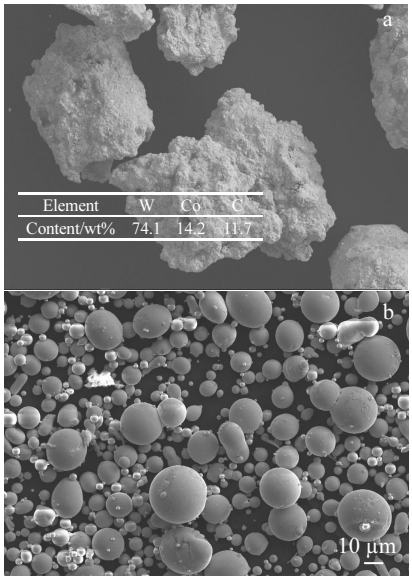

Fig.1 Morphologies of coating powder: (a) WC-12Co and (b) Ni60

Table 1 Chemical composition of Ni60 and Ni25 alloy (wt%)

Alloy	C	Cr	Si	B	Fe	Ni
Ni25	0.1	-	3.8	1.5	6.8	Bal.
Ni60	0.2	17.5	4.0	3.0	12.5	Bal.

The spot diameter was 5 mm. The overlapping ratio was 40%. Before the experiment, the Ni60 and Ni25 powder were dried at 120 °C in a vacuum oven for 60 min. The WC-12Co and Ni25 powder were synchronously injected into the laser molten pool using double tube powder feeder. The process parameters for preparing the coatings are given in Table 2.

In order to investigate the microstructure of Ni60 coating and WC-12Co/Ni25 composite coating, the cross-section coating specimens were cut by wire electrical discharge machining. The specimens ground and polished into a mirror were etched with a corrosive solution of 30 mL HCl:10 mL HNO_3:2 g $FeCl_3$ for 5 s. The microstructure, phase composition, element distribution and worn track of coatings were analyzed by scanning electron microscopy (SEM, JSM-6700), energy dispersive spectrum (EDS, OXFORD 6650) and X-ray diffraction (XRD, D8 ADVANCE).

The hardness of the coatings was measured along the thickness direction of the coating under a load of 4.9 N using a Vickers micro-hardness tester (HMV-2T). The wear resistance tests were carried out by a pin-on-disk wear test machine (MS-T3001) at room temperature under dry sliding condition. The pin was a Si_3N_4 ceramic ball with 5 mm in diameter. The disk was the coating specimen which was polished, cleaned in an ultrasonic bath, and finally dried. The test was performed under a normal load of 500 g at a rotation speed of 1000 r/min. The radius of wear track was 4 mm. The cross-section profile of worn tracks was measured by a step profiler (MFT-4000), and the abrasive loss was evaluated by sectional area and perimeter of worn tracks.

2 Results and Discussion

2.1 Microstructure

The Ni60 coating (specimen 1) and WC-12Co/Ni25 composite coating (specimen 2) were deposited on the W1813N steel substrate using laser cladding. The microstructure of specimens 1 and 2 are presented in Fig.2a and 2b, respectively. It is obvious that the bonding interface of both specimen 1 and specimen 2 is smooth and compact, which implies the less dilution of substrate. In Fig.2a, the white zone with a thickness of 200~300 μm at the coating/substrate interface should be the heat affected zone (HAZ) resulting from self-quenching of laser irradiation. The microstructure at the bottom of Ni60 coating is dendrite perpendicular to substrate against the direction of heat dissipation, and the microstructure at the middle of Ni60 specimen is fine equiaxed crystal, as shown in Fig.2c.

As shown in Fig.2b, the WC-12Co particles are uniformly distributed in the Ni25 matrix, and the volume fraction of WC-12Co in the composite coating is 32.5 vol%. The bonding interface of WC-12Co particle in Ni25 matrix shows that there is good compatibility, as seen from Fig.2d.

In order to analyze the interface dilution of specimen 1, the line scanning of Si, Cr, Fe and Ni elements from Ni60 coating to substrate was carried out by EDS in the cross-section of specimen 1, and the results of elemental concentration are illustrated in Fig.2e. It can be seen that the transient region of elements is only 10~15 μm, which suggests that the white zone in the bonding interface of specimen 1 is not a dilution zone but a heat affected zone (HAZ). In addition, the line scanning from Ni25 matrix to WC-12Co particle was performed by EDS along the black line in Fig.2d, and the contents of Ni, Fe and W elements drop down and rise up straightly from Ni25 to WC-12Co particle, as illustrated in Fig.2f. The results indicate that there is no obvious transition layer at WC-12Co/Ni25 interface.

Table 2 LC parameters of Ni60 and WC-12Co/Ni25 coatings

Specimen	Feeding rate/ $g \cdot min^{-1}$	Scanning velocity/ $mm \cdot s^{-1}$	Laser power/ kW
Ni60	15	8	4
WC-12Co/Ni25	12	8	4.2

2.2 Phases of microstructures

The XRD analysis was performed on Ni60 coating and WC-12Co/Ni25 composite coating, as presented in Fig.3. The analysis was operated at 40 kV and 40 mA to generate monochromatic Cu Kα radiation with a wavelength of 0.154 056 nm. It can be seen that γ-Ni and FeNi solid solution are the main matrix phases, while $Cr_{23}C_6$, Cr_2B and Fe_5C_2 are the main strengthening phases in the LC Ni60 coating, as indicated in Fig.3a. The phases of the LC WC-12Co/Ni25 composite coating are distinctly different from that of the Ni60 coating due to the addition of WC-12Co particles. The XRD results in Fig.3b demonstrate that γ-Ni, FeNi solid solution and Co are the main matrix phases, while the WC, $FeSi_2$, NiSi and SiC are the main strengthening phases. According to the above results of two coatings, the hardness and wear resistance of the LC Ni60 coating are directly related to $Cr_{23}C_6$ and Cr_2B, while the hardness and wear resistance of the LC WC-12Co/Ni25 composite coating should be mainly related to the WC particles.

2.3 Hardness of coatings

The micro-hardness variation curves of the Ni25, Ni60 and WC-12Co/Ni25 coatings are presented in Fig.4. According to descriptive statistics, the mean microhardness of the Ni25, Ni60 and WC-12Co/Ni25 coatings are 3660, 6540 and 6780 MPa, respectively. The hardness distribution of Ni25 and Ni60 coatings is relatively uniform and stable, and the standard deviations of both the coatings are much smaller than the standard deviation 220 of composite coating. Meanwhile, in the WC-12Co/Ni25 composite coating, the minimum, medium and maximum microharnesses are 3920, 6110 and 10 400 MPa, respectively, in which the difference value between minimum and maximum microhardness reaches 6480 MPa. It can be seen that the minimum microhardness is close to the microhardness of Ni25 coating, while the maximum microhardness is tested in the WC-12Co particles. However, the mean microhardness of the Ni60 and WC-12Co/Ni25 coatings is even close to each other.

2.4 Wear resistance

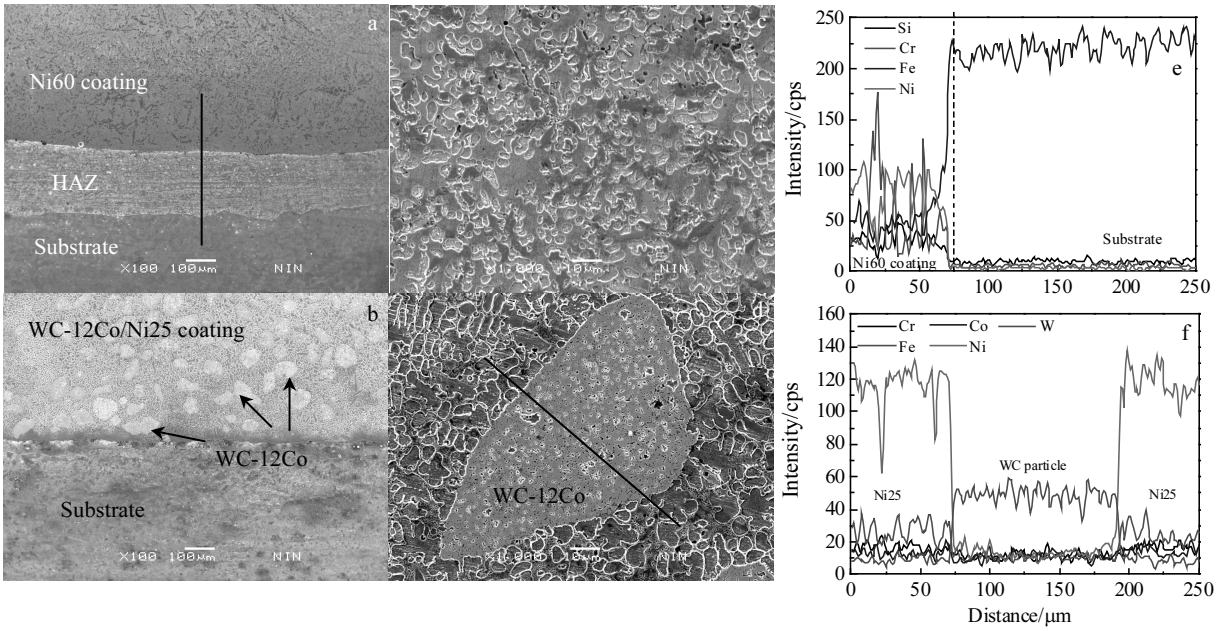

Fig.2 Cross-sectional SEM microstructure of coatings: (a) bonding interface of Ni60 coating, (b) bonding interface of WC-12Co/Ni25 composite coating, (c) Ni60 coating, (d) WC-12Co/Ni25 composite coating; EDS element linear scanning from Ni60 coating to substrate (e) and Ni25 to WC-12Co particle (f)

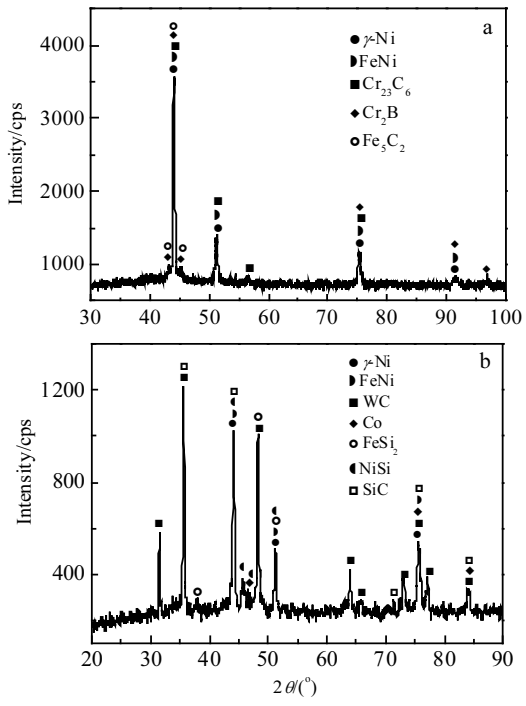

Fig.3 XRD patterns of coatings prepared by laser cladding: (a) Ni60 coating and (b) WC-12Co/Ni25 composite coating

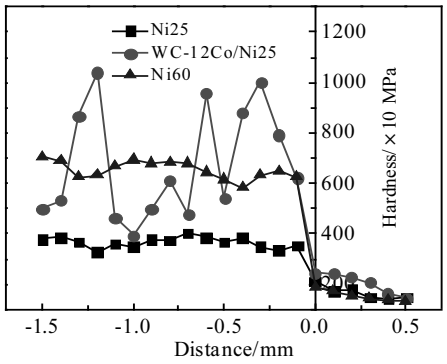

Fig.4 Micro-hardness profiles of LC Ni60, Ni25 and WC-12Co/Ni25 coatings

Pin-on-disc wear test was performed on the LC Ni60 and WC-12Co/Ni25 coatings at room temperature in atmospheric environment and dry sliding condition. According to the test parameters (Section 2.3), the cumulative sliding distance of the Si_3N_4 ceramic ball on the coatings is about 7536 m. The sliding linear velocity is about 0.418 m/s. The evolution of friction coefficient of the coatings was recorded during the wear process, as presented in Fig.5. As shown, the friction coefficient of the composite coating is smaller and more stable than that of the Ni60 coating. In order to accurately evaluate the friction coefficient of the coatings, the coefficient of sliding for about 30 min in the initial running-in stage should not be calculated. In consequence, the mean friction coefficient of the Ni60 coating is about 0.64 ± 0.02, while the mean coefficient of the composite coating is about 0.56 ± 0.01 after 300 min sliding. The maximum coefficients of the Ni60 coating and composite coating are 0.69 and 0.59, respectively. This demonstrates that the reduction in friction coefficient of the

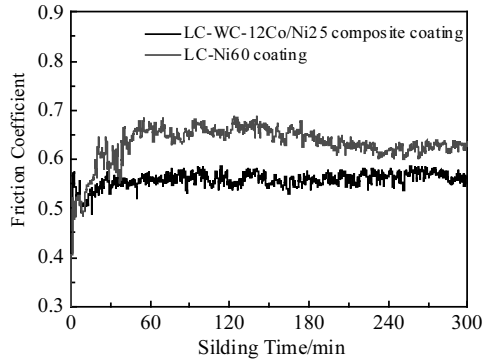

Fig.5 Variation curves of friction coefficient with sliding time

composite coating can be attributed to the WC-12Co ceramic particles which are uniformly embedded in soft Ni25 matrix.

In order to evaluate the abrasion loss, a step profiler was used to measure the depth of worn scratch and the cross profile of wear track using the scriber which moves uniformly along a straight line with the loading of 0.05 N on the surface of worn track, as shown in Fig.6. The volume loss was estimated by the volume of the wear track, which is the area of the cross profile multiplied by the periphery of the wear track. The cross-sectional area of the wear track was measured at four locations along each wear tracks (named 1#~4#), and the mean value was used to calculate the volume of the wear track. The loss of the two coatings is listed in Table 3. Obviously, the volume loss of the LC WC-12Co/Ni25 is only 10% of that of the LC Ni60, which suggests that the WC-12Co/Ni25 coating exhibits better wear resistance.

To further analyze wear failure behavior of worn tracks, the worn surfaces of the coatings were investigated using SEM and EDS, and the results are shown in Fig.7. It can be seen that the wear track of the Ni60 coating has obviously deeper scars and plough than that of the composite coating; the width of the wear track of the Ni60 coating is wider than that of the composite coating. From Fig.7b, the WC-12Co particles are uniformly distributed on the surface of composite coating. There are dark adhesive scraps on both worn coating surfaces. The EDS analysis was performed on the dark scraps of wear track of the LC Ni60 and WC-12Co/Ni25 coatings, and the results are presented in Fig.7e and 7f. It can be seen that the dark scraps (spectrum 2 and 4) have higher content of O than the light matrix (spectrum 1 and 3). In addition, the spectrum 5 was performed on WC-12Co particles according to the high content of W. The Co content of spectrum 3 is higher than that of spectrum 5. This implies that oxidation occurs in the dark areas of worn track when the coating specimens are subjected to sliding wear tests. The higher Co content in the spectrum 3 indicates that Co element from the WC particles is prone to melting in the Ni25 matrix in the laser cladding process.

2.5 Discussion

The Ni60 (60 HRC) and Ni25 (25 HRC) alloys are representative of hard and soft Ni-based self-fluxing alloy, respectively, and the difference of them is attributed to the existence of Cr element. Part of Cr added in the Ni-based alloy is used for solid solution strengthening, and then excessive Cr can react with C and B elements to produce Cr carbides and borides[7,10,17]. The hardness enhancement of the Ni-based self-fluxing alloy is attributed to the existence of more hard CrB ceramics and Cr_mC_n carbides phases, which is also consistent with the results reported by Yao[11]. The crystalline grains of the LC Ni60 microstructure are mainly γ-Ni/FeNi solid solution, while the hard Cr_mC_n and Cr_2B phases are concentrated at the grain boundary.

The Ni60 alloy with excellent wear resistance, oxidation resistance and corrosion resistance is one of primary wear materials, but it cannot meet the wear resistance requirements of oil

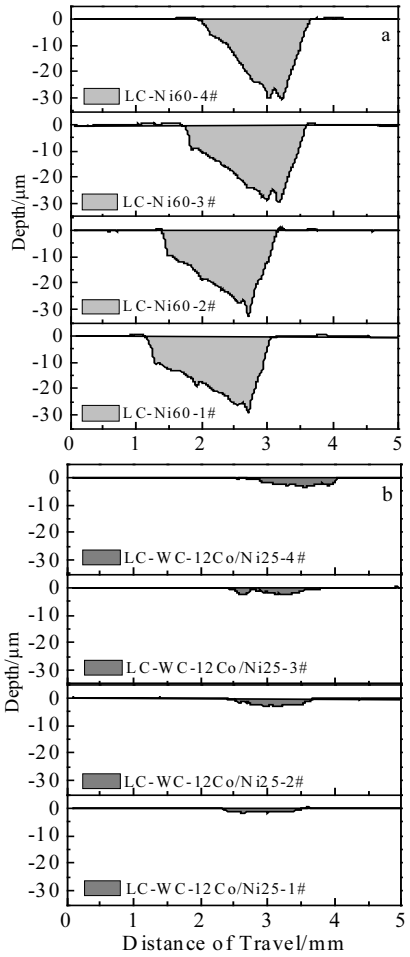

Fig.6 Cross-sectional profiles at four locations of worn tracks: (a) Ni60 coating and (b) WC-12Co/Ni25 composite coating

Table 3 Wear test results of the Ni60 and WC-12Co/Ni25 coatings

Coat	Volume loss/mm^3	Maximum depth of wear track/μm	Mean width of wear track/mm
Ni60	0.74± 0.13	30.8 ± 2.2	1.73 ± 0.09
WC-12Co/Ni25	0.07± 0.03	4 ± 0.8	1.44 ± 0.08

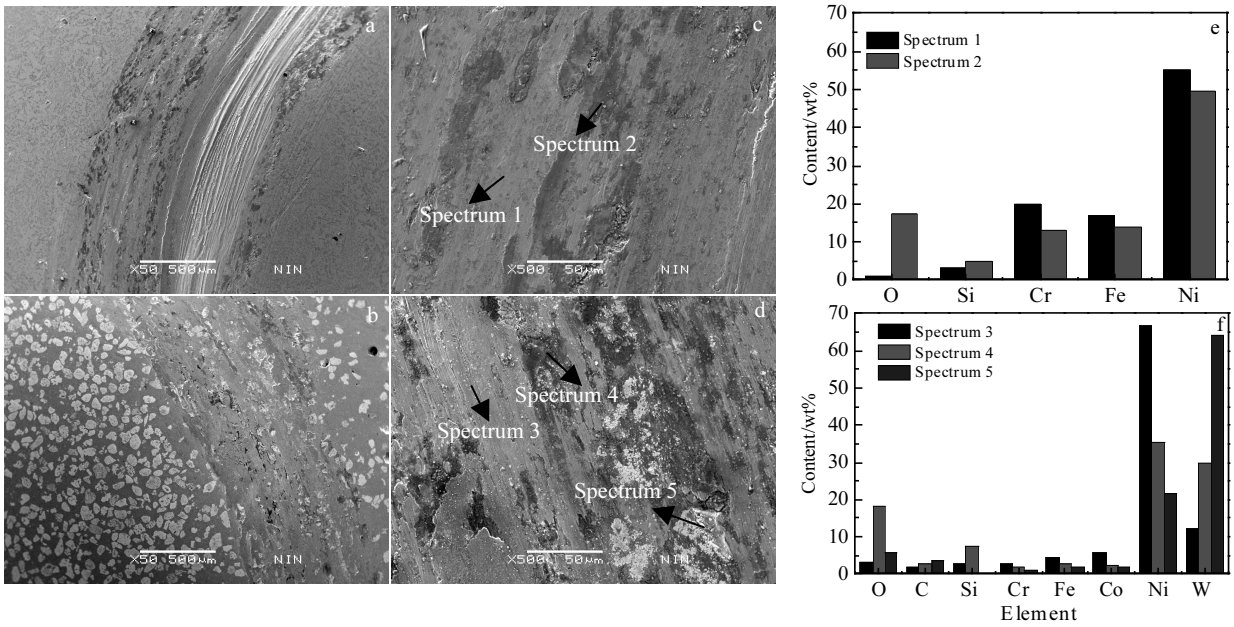

Fig.7 SEM morphologies (a~d) and EDS analysis (e, f) of worn surfaces: (a, c, e) Ni60 coating and (b, d, f) WC-12Co/Ni25 composite coating

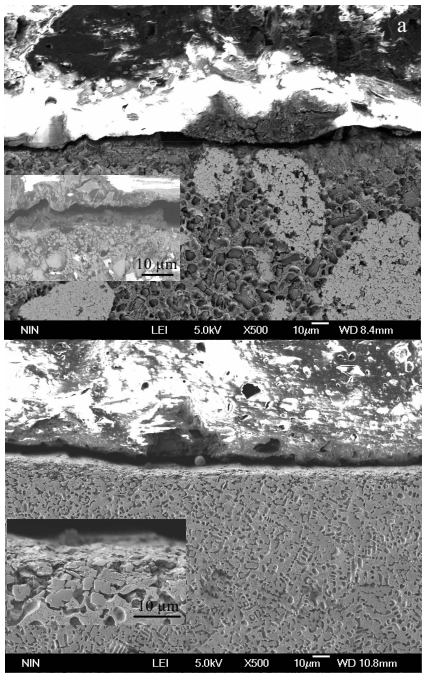

Fig.8 Cross-sectional SEM images of worn tracks: (a) WC-12Co/Ni25 coating and (b) Ni60 coating

industry. WC ceramics with excellent hardness and thermostability are usually used as enhancement phase. However, the WC ceramic particles added in the hard Ni60 coating will generate serious cracking, so the soft and ductile Ni25 alloy like a sponge is applied to be bonding matrix of WC-12Co to assimilate the composite coating stress. Due to the best wettability of Co and WC, the WC particles are protected by the Co metal with good thermal and oxidative stability. The WC-12Co particles have good toughness and ablation resistance compared to WC. The Co element can also increase the interface bonding strength between WC and Ni25 alloy.

According to the microstructures, phases and hardness results of Ni60 and WC-12Co/Ni25 coatings, the $Cr_{23}C_6$ and Cr_2B hard phases in the LC Ni60 coating usually accumulate in the crystal boundary of γ-Ni solution, while in the WC-12Co/Ni25 composite coating, the WC-12Co particles are firmly embedded in the Ni25 matrix. When the Si_3N_4 pin is sliding relative to the coatings under vertical loading, the tiny $Cr_{23}C_6$ and Cr_2B phases in the grain boundary of Ni60 coating are not enough to resist the scratching. On the contrary, the big WC-12Co particles can support the composite coating to protect the soft Ni25 matrix.

According to the abrasion loss and profiles of wear tracks, the surface abrasion behaviors of the LC Ni60 coating is ploughed shape and adhesive scrap, but the surface abrasive behaviors of the LC WC-12Co/Ni25 composite coating are adhesive scraps and WC debris. Fig.8 presents the cross-sectional SEM images of worn tracks. In Fig.8a, there is a plastic flow of the Ni25 matrix at the top of cross-sectional SEM microstructure of the WC-12Co/Ni25 coating. In Fig.8b, there is also a compressive deformation layer of microstructure at the top of cross-sectional SEM image of the Ni60 coating. It demonstrates that there are plastic rheological behaviors of Ni60 and Ni25 matrix in sliding process. Therefore, the main wear mechanism of the Ni60 coating is abrasive wear and adhesive wear, while the main wear mechanism of the WC-12Co/Ni25 coating is adhesive wear.

3 Conclusions

1) In the LC Ni60 coating, the microstructure is mainly fine

dendrites and equiaxed crystals, and the hard $Cr_{23}C_6$ and Cr_2B phases are distributed in the grain boundaries of γ-Ni and FeNi solid solution. In the composite coating, WC-12Co particles are uniformly embedded in the γ-Ni and FeNi solid solution.

2) The mean hardness of the LC Ni60 and WC-12Co/Ni25 coatings is 6540 ± 350 MPa and 6780 ± 2200 MPa, respectively. The hardness distribution of Ni60 coatings is relatively uniform and stable. However, the difference value between minimum and maximum hardness of the WC-12Co/Ni25 composite coating reaches 6480 MPa.

3) The mean coefficients of the two coatings are similar, but the volume loss of the LC WC-12Co/Ni25 is only 10% of that of the LC Ni60. The surface abrasive characters of the LC Ni60 coating are ploughed shape and adhesive scraps, but the surface abrasive characters of the LC WC-12Co/Ni25 composite coating are adhesive scraps and WC debris. The main wear mechanism of the Ni60 coating is abrasive wear and adhesive wear, while the main wear mechanism of the WC-12Co/Ni25 coating is adhesive wear. These demonstrate that the WC-12Co/Ni25 coating exhibits better wear resistance.

References

1 Lin Q S, Zhou K S, Deng C M *et al. Journal of Thermal Spray Technology* [J], 2014, 23(6): 892

2 Bolelli G, Berger L M, Borner T *et al. Surface and Coatings Technology*[J], 2015, 265: 125

3 Yazdani Z, Karimzadeh F, Abbasi M H *et al. Transactions of the Indian Institute Metals*[J], 2015, 68(5): 927

4 Weng F, Chen C, Yu H. *Materials & Design*[J], 2014, 58(6): 412

5 Bai L L, Li J, Chen J L *et al. Optics & Laser Technology*[J], 2016, 76: 33

6 Simunovic K, Saric T, Simunovic G. *Tribology Transactions*[J], 2014, 57(6): 955

7 Xuan H F, Wang Q Y, Bai S L *et al. Surface & Coatings Technology*[J], 2014, 244(15): 203

8 Li J F, Cheng J G, Chen P Q *et al. Ceramics International*[J], 2018, 44(10): 11 225

9 Pellan M, Lay S, Missiaen J M *et al. Acta Materialia*[J], 2018, 155: 372

10 Wang C, Gao Y, Wang R *et al. Journal of Alloys & Compounds*[J], 2018, 740: 1099

11 Yao J H, Yang L J, Li B *et al. Materials & Design*[J], 2015, 83: 26

12 Sui Y Y, Yang F, Qin G L *et al. Journal of Materials Processing Technology*[J], 2018, 252: 217

13 Shu D, Li Z G, Zhang K *et al. Materials Letters*[J], 2017, 195: 178

14 Yao J H, Zhang J, Wu G L *et al. Optics & Laser Technology*[J], 2018, 101: 520

15 Ma Q, Li Y, Wang J. *International Journal of Refractory Metals & Hard Materials*[J], 2017, 64: 225

16 Deschuyteneer D, Petit F, Gonon M *et al. Surface & Coatings Technology*[J], 2015, 283: 162

17 Ismail Hemmati, Václav Ocelík, Kornel Csach *et al. Metallurgical & Materials Transactions A*[J], 2014, 45(2): 878

W1813N 无磁不锈钢表面激光熔覆 Ni60 与 WC-12Co/Ni25 涂层的组织结构和磨损行为

杨理京，张平祥，王少鹏，李争显，王 培，李 欢，杨海彧

(西北有色金属研究院，陕西 西安 710016)

摘 要：利用激光熔覆技术在 W1813N 无磁性不锈钢表面分别制备高硬度镍基自熔性合金 Ni60（60HRC）涂层和低硬度 Ni25 基 WC-12Co 复合涂层。利用扫描电子显微镜（SEM）、能谱（EDS）、X 射线衍射仪（XRD）和台阶仪，分析激光熔覆制备 Ni60 涂层和 WC-12Co/Ni25 复合涂层的显微组织、相组成和磨损行为。利用显微硬度、摩擦系数、磨痕轮廓对比 2 种涂层的耐磨性和磨损机制。结果表明，Ni60 涂层显微组织主要为树枝晶和等轴晶，且 $Cr_{23}C_6$, Cr_2B 等强化相弥散分布在γ-Ni 和 FeNi 固溶体晶界；而 WC-12Co/Ni25 复合涂层中 WC-12Co 颗粒弥散镶嵌于低硬度 Ni25 基质，复合涂层中 WC-12Co 颗粒体积分数达到 32.5 vol%。复合涂层中最大和最小显微硬度差异达到 6480 MPa。尽管 2 种涂层的摩擦系数相近，但复合涂层的磨损体积仅为 Ni60 涂层的 10%，Ni60 涂层表面的磨痕特征为犁沟状和塑性粘附，复合涂层磨痕表面为 WC 碎屑和塑性粘附，因此 Ni60 涂层的磨损机制为磨粒磨损和粘着磨损，而复合涂层磨损机制为粘着磨损。以上结果表明 WC-12Co/Ni25 复合涂层具有更好的耐磨性。

关键词：镍基合金；WC-12Co陶瓷；激光熔覆；复合涂层；耐磨性

作者简介：杨理京，男，1984 年生，博士，高级工程师，西北有色金属研究院，陕西 西安 710016，E-mail: yanglijing84@126.com